Towards Simulation of Clogging Effects in Wastewater Pumps: Modelling of Fluid Forces on a Fiber of Bonded Particles using a Coupled CFD-DEM Approach

Anna Lyhne Jensen*[1], Henrik Sørensen[1], Lasse Rosendahl[1]

ISROMAC 2016

International Symposium on Transport Phenomena and Dynamics of Rotating Machinery

Hawaii, Honolulu

April 10-15, 2016

Abstract

Clogging in wastewater pumps is often caused by textile and other fibrous materials in the wastewater. As a step towards developing a methodology using the CFD-DEM approach for simulation of clogging effects, a fiber model consisting of a string of bonded DEM particles is developed in the software EDEM and coupled (two-way momentum exchange) to the CFD software ANSYS Fluent. The number of particle segments forming the fiber as well as the properties of fiber density and fiber stiffness are changed to identify the influnce of these properties on the fiber motion in shear flow. A change of density from 500 kg/m^3 to 5000 kg/m^3 strongly affects the motion of the fiber, while a change of the stiffness of the bonds between the spherical particles from 1e^7 to 1e^9 has less influence on the fiber motion. The results of using 20 and 50 fiber segments respectively are similar in the first period of simulation, but the deviation between the two cases increase with time. The difference may be caused by the difference in fiber aspect ratio in the two cases. The influence of fiber properties on fiber motion has been analysed quantitatively and compared to fiber orbit types presented in literature [8],[11]. The results show that fiber motion similar to the motion presented in literature is obtained using a coupling between EDEM and ANSYS Fluent.

Keywords

CFD-DEM — Clogging — Fiber Modelling — Shear Flow

[1] *Department of Energy Technology, Aalborg University, Denmark*

*__Corresponding author__: alj@et.aau.dk

INTRODUCTION

Clogging in wastewater pumps, due to objects such as textiles and plastic in wastewater, causes severe problems in wastewater pumping systems. Therefore, resilience to clogging is a key requirement in the design of wastewater pumps. The design process of wastewater pumps is commonly based on empirical knowledge and expensive and time consuming experiments on prototypes. Thus, a method for simulating clogging effects will significantly facilitate the design process.

Computational Fluid Dynamics (CFD) is widely used in the design process of pumps. However, simulation of clogging effects entails simulation of the objects in the wastewater causing clogging, such as plastic bags or textile. This fact significantly complicates the simulation, and therefore simulation of clogging effects in wastewater pumps has not previously been done. Different applicable approaches for simulation of the interaction between fluid and flexible materials exist. These include the Immersed Boundary Method [1], the Arbitrary Lagrangian-Eulerian method [2], Smoothed Particle Hydrodynamics coupled with the Finite Element Method [3] and coupled CFD-DEM, which has been discussed in [4]. Advantages of using the CFD-DEM approach are that self-collision of the textile can be handled by the DEM soft-sphere collision model. Furthermore, it is advantageous that dynamic meshing is not required, since the DEM particles are not resolved by the CFD mesh. In the present study, a flexible fiber in shear flow is modeled using the DEM software EDEM from DEM Solutions in a two-way coupling to the CFD software ANSYS Fluent including fibre self-interactions. This model is the first step towards developing a CFD-DEM framework for simulation of flexible pieces of textile and the interaction of the textile with fluid applicable for simulation of clogging effects.

Bonded Discrete Elements DEM was introduced by Cundall and Strack (1979) [5] for the simulation of solid flows with mechanical transport. The method computes the motion of a large number of particles of finite size using Newtons 2. law of motion as given in Eq. (1) and (2)

$$m_\mathrm{i}\vec{a}_\mathrm{i} = \vec{F}_\mathrm{i,n} + \vec{F}_\mathrm{i,t} + \vec{F}_\mathrm{i,b}\,, \tag{1}$$

$$I_\mathrm{i}\vec{\alpha}_\mathrm{i} = \vec{r}_\mathrm{i,c} \times \vec{F}_\mathrm{i,t}\,, \tag{2}$$

where m_i is the mass and a_i is the acceleration of the i^th particle. $F_\mathrm{i,n}$ and $F_\mathrm{i,t}$ are the normal and tangential particle-particle contact forces and $F_\mathrm{i,b}$ is additional forces as gravity and fluid force. In Eq. 2, I_i and $\vec{\alpha}_\mathrm{i}$ are the moment of inertia and the angular acceleration of the i^{th} particle respectively, and $r_\mathrm{i,c}$ is a vector from the center of the particle to the point where the force $F_\mathrm{i,t}$ acts.

When modeling a fiber as a chain of bonded spherical DEM particles, a second model for particle-particle interaction of the bonded particles must be introduced. Since the fiber is not completely flexible, normal and shear stiffness of the fiber are introduced in the model of the bonds between the

particles. Thus, bonded particles resist normal and tangential displacements. Furthermore, the bond breaks if a specified normal or tangential limit for stress is exceeded. Existing bond models in DEM have primarily been developed for simulation of rock and concrete. This also applies to the build in bond model in the software EDEM, "Hertz-Mindllin with bonding", which is a modification of the bond model for rock proposed by Potyondy and Cundall (2004) [6]. Guo et al. (2013) [7] used DEM to model flexible fibers. The bond model used by Guo et al. (2013) was also based on the bond model proposed [6] and the results showed good correspondence between theory and model. Further validation of the bond model in EDEM for the use for flexible fibers is necessary, but out of scope of this paper.

Fig. 1 illustrates a bond between two particles of a fiber. A bond is formed if the contact radii r_c of two particles overlap. The radius r is the particle radius and is used for force calculation between particles.

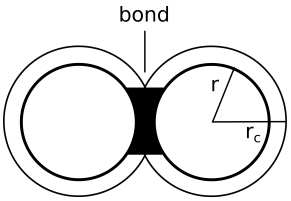

Figure 1. The particle radius, r, and the contact radius r_c is defined when modeling bonded particles. Bonds are formed if there is particle contact within the radius r_c. Bond properties include normal and shear stiffness of the bond and critical shear and normal stress break criteria.

Flexible Fibers in Shear Flow The DEM fiber model will be coupled to a CFD simulation of shear flow as sketched in Fig. 2.

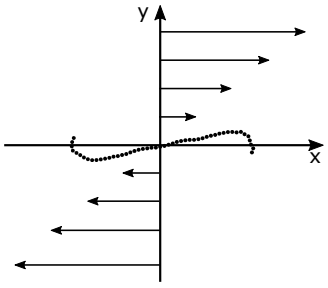

Figure 2. Flexible fiber orbiting in shear flow.

Previous work on fibers in shear flow includes Forgacs and Mason (1959) [8], who investigated the motion of flexible wood-pulp fibers in shear suspensions experimentally. More recently, the motion has been modeled by Yamamoto and Matsuoka (1993) [9] and Schmid et al. (2000) [10] by dividing the fiber into spherical and cylindrical bonded segments respectively, and modelling the hydrodynamic force on these segments. Lindström et al. (2007) [11] also modeled fibers as chains of cylindrical fiber segments. In this model the flow was modeled by 3D incompressible Navier-Stokes equations using a two-way coupling between the fiber and the fluid. The model took into account both viscous and dynamic drag forces. An important conclusion of the work was that fiber motion cannot be described without taking two-way coupling into account. Based on this, a two-way coupling between the fluid and the fiber is implemented in the present work.

Different orbit types depending on the flexibility of the fiber was characterized by Forgacs and Mason (1959) [8]. These are rigid orbits, springy orbits, snake orbits and coiled orbits. These orbit types are sketched in Figure 3. The stiffness of the fiber increases from the coiled orbit type down to the rigid orbit type. Notice from the figure that rigid, springy and snake orbits are periodic. The present simulation of fibers in shear flow in EDEM and ANSYS Fluent is validated by qualitatively comparing the results to the different orbit regimes by [8], [11].

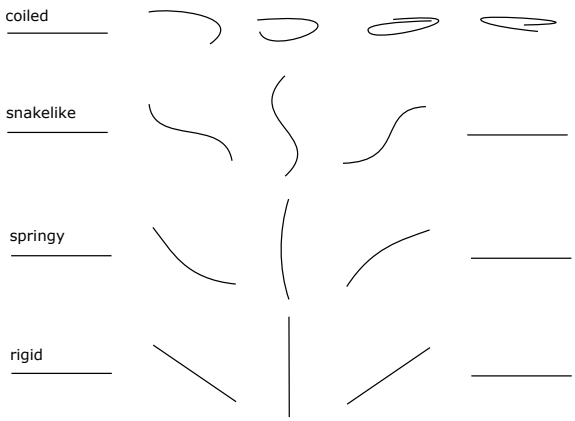

Figure 3. Sketch of four different orbit types of fibres in shear flow: rigid, springy, snakelike and coiled [8],[11].

The diameter of fibers in pulp and paper industry is in the order of 10^{-5}m. The aim of this work is to simulate one yarn of a floor cloth which has a diameter in the order of 10^{-3}m. Therefore the size scale differs significantly, but it is expected that the yarn will orbit in a way similar to that of the fibers. The fiber stiffness, density and the number of particles forming the fiber are changed, and the influence of these changes on the fiber motion is investigated to assess the applicability of the present bond model and coupling in EDEM and ANSYS Fluent, to simulation of flexible fibers or textiles in fluid flow.

1. METHODS

Navier-Stokes equations for an incompressible fluid with particles are given in Eq. (3) and Eq. (4) [12]

$$\frac{\partial \alpha_f}{\partial t} + \nabla \cdot (\alpha_f \vec{u}_f) = 0\,, \tag{3}$$

$$\frac{\partial (\alpha_f \vec{u}_f)}{\partial t} + \nabla \cdot (\alpha_f \vec{u}_f \vec{u}_f) = -\alpha_f \nabla \frac{p}{\rho_f} - \vec{R}_{pf} + \nabla \cdot \tau\,, \tag{4}$$

where α_f, $\vec{u}_f$ and ρ_f is the is the fluid volume fraction, fluid velocity and fluid density respectively. $\tau = \nu_f \nabla \vec{u}_f$ is the fluid

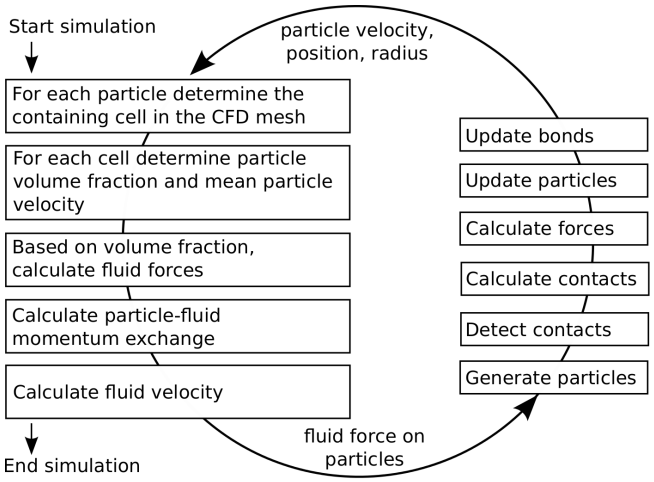

Figure 4. Block diagram of calculation process in a coupled CFD-DEM simulation. The blocks to the left represent the CFD solver and the blocks to the right represent the DEM solver.

phase stress tensor and $\vec{R}_{\mathrm{pf}}$ is the fluid-particle momentum exchange. Figure 4 illustrates the calculation steps in a coupled CFD-DEM simulation. The simulation starts in the CFD solver, which calls the DEM solver. In the CFD solver the containing cell of each particle is identified and the the particle volume fraction in each cell is determined. Based on the volume fraction, the fluid force in each cell can be determined. In the present work, this corresponds to the drag force. Finally, the CFD solver determines the particle-fluid momentum exchange and the fluid velocity before the fluid force is transferred to the DEM solver. The CFD time step is larger than the DEM time step and thus the DEM calculations are repeated until the time which corresponds to a CFD time step have been completed. Then the velocity, position and radius of all particles are transferred to the CFD solver.

1.1 Domain and Boundary Conditions

The domain and boundary conditions used in CFD are presented in Fig. 5. Periodic boundary conditions are used in the right and left part of the domain and symmetry is used on the front and back of the domain. The moving walls in the upper and lower part of the domain create a shear flow as sketched in Fig. 2. The velocity profile is linear and is given by Eq. 5

$$v_{\mathrm{x}} = a \cdot y\,, \tag{5}$$

where v_{x} is the velocity in the $x-$direction and y is the position on the $y-$axis. A constant value of $a = 2.5$ is used in all the described simulations, and the role of shear rate will not be investigated. Furthermore, gravity is not included in the simulation.

The domain is meshed with hexahedral cells of equal size. The ratio between the particle volume and cell volume is approximately 1/15.

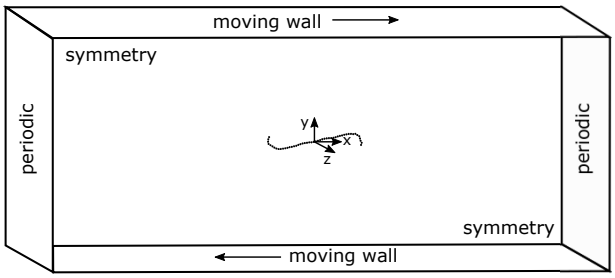

Figure 5. CFD domain. The upper and lower boundaries are moving walls with no slip. This creates a shear flow in the domain. The right and left part of the domain has periodic boundary conditions. The fiber of DEM particles orbits in the center of the domain.

1.2 Fiber Model

The model of the mechanics of fibers include particle-particle interaction through bonds or collision, and drag force on the fiber. Morphological properties of the fiber such as length and diameter as well as the fiber stiffness and density are expected to have a major influence on resulting fiber orbit types. These parameters are varied and the influence on the fiber motion is evaluated. The diameter of the spherical particle segments forming the fiber is 2.5 mm, to resemble the size of the yarns of a woven floor cloth. The contact radius is set to be 20 % larger than the particle radius. Furthermore, the number of particle segments forming the fiber is 20 or 50, resulting in aspect ratios of 20 and 50 respectively. Fiber aspect ratios between 50 and 780 were investigated by [8], [10] and [13].

1.3 Drag Model

Using the CFD-DEM approach, the bonded particles are not resolved by the CFD mesh. Therefore a drag law must be ascribed to the particles. The coupling framework for EDEM and Fluent includes a freestream drag formulation as well as formulations of drag developed by Ergun (1952) [14] and Wen and Yu (1966) [15] and di Felice (1994) [16] for fluid particle interaction in packed and fluidized beds. No drag formulation for the modeling of bonded particles is available. In the freestream drag formulation, the drag coefficient depends on the Reynolds number. The Reynolds number is based on the particle diameter, d_{p}, and is calculated as given in Eq. 6.

$$Re = \frac{\rho_{\mathrm{f}} \cdot v_{\mathrm{rel}} \cdot d_{\mathrm{p}}}{\mu_{\mathrm{f}}} \tag{6}$$

Where v_{rel} is the relative fluid velocity, and ρ_{f} and μ_{f} are the fluid density and viscosity respectively. The drag coefficient is calculated based on the classical formulation of drag on a sphere, using Eq. 7.

$$c_{\mathrm{d}} = \begin{cases} 24/Re, & \text{if } Re \leq 0.5; \\ 24 \cdot \left(1 + 0.15 \cdot Re^{0.687}\right)/Re, & \text{if } 0.5 < Re \leq 1000; \\ 0.44, & \text{otherwise.} \end{cases} \tag{7}$$

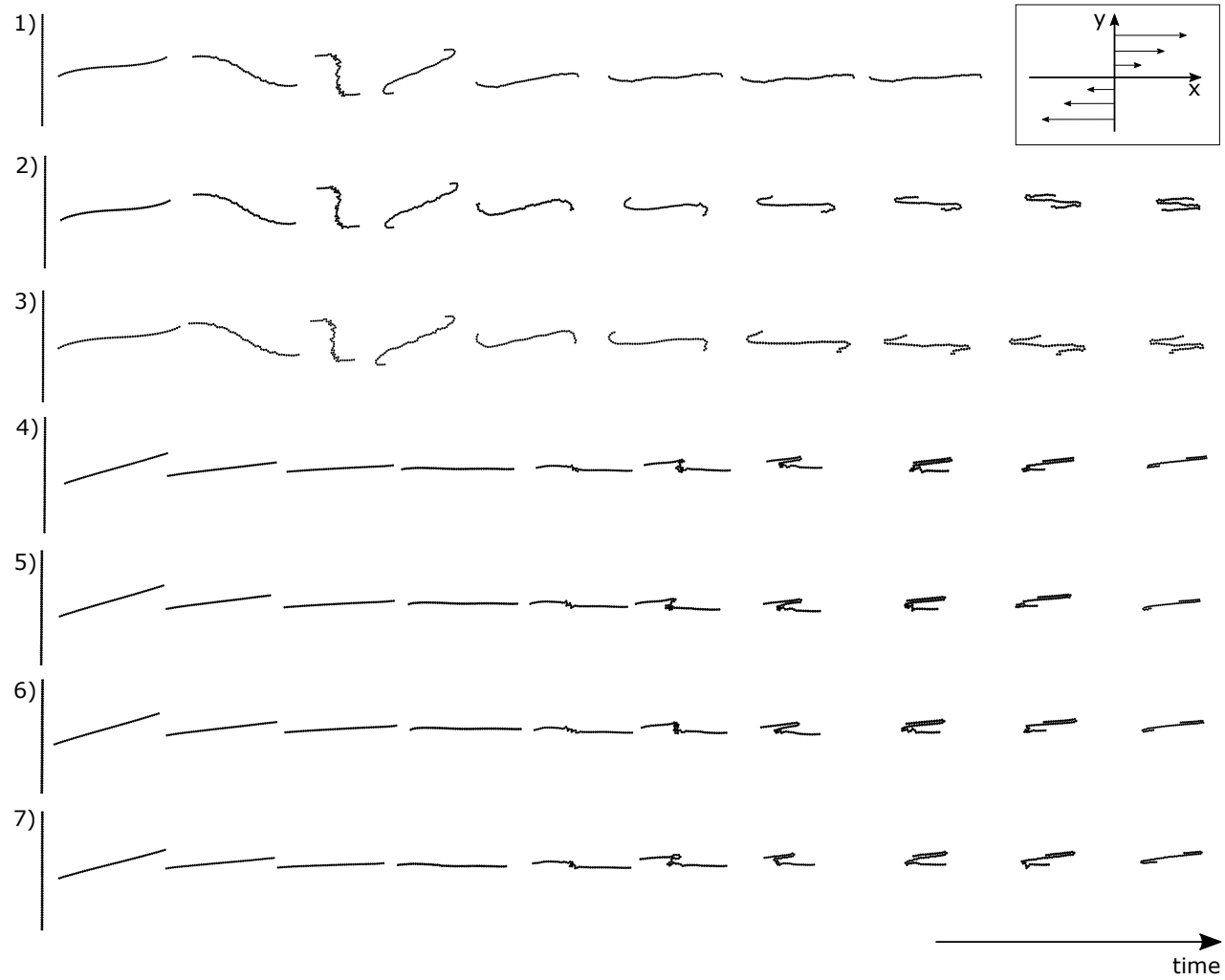

Figure 6. Development of the fiber shape with time in the different cases. The time interval between each image in a case is 1 s.

Using the drag coefficients determined for each particle by Eq. 7, the drag force on each particle of the fiber can be calculated by Eq. 8

$$F_{\mathrm{d}} = 0.5 \cdot c_{\mathrm{d}} \cdot \rho_{\mathrm{f}} \cdot A \cdot v_{\mathrm{rel}}\,, \tag{8}$$

where A is the particle area. The viscosity of the water is 0.001003 kg/m·s and the density is 998.2 kg/m^3. The drag force on the particles is used to determine the particle-fluid momentum exchange.

2. RESULTS AND DISCUSSION

13 different fibers were simulated by varying the fiber density, bond shear and normal stiffness and number of fiber segments. The initial orientation of the fiber is vertical, perpendicular to the flow direction. The results are presented in Fig. 6 for a fiber formed by 50 segments and in Fig. 7 for a fiber formed by 20 segments. The figures show the initial state of the fiber and 10 following states. The time interval between the fibers in each case is 1 s. The properties of the fiber in each of the cases shown in Fig. 6 are listed in Tab. 1. Note that since the fiber consists of spherical particles, the aspect ratio of the fiber is equal to the number of particle segments.

The movement of the fibers in case 1-3 is very similar, especially for the first 4 s. Common for the three fibers is the density of 5000 kg/m^3, which gives a density ratio between the fibers and the fluid close to 5. The difference between the three cases is the fiber stiffness. The fiber in the first case is the most flexible. This is evident from the results where the shear flow causes the fiber to continue the rotation in an orbit which resembles a cross between the snakelike motion and the coiled motion sketched in Fig. 3. The least flexible fiber (case 1), stops rotating in the area of low fluid velocity in the center of the domain.

A standard floor cloth has a dry density of around 150 kg/m^3. When submersed in water the cloth will absorb water and the wet density of the cloth will be higher than the dry density. In case 4-6 it is assumed that the wet density of the cloth is around 500 kg/m^3, and in the 7$^{\mathrm{th}}$ case the fiber and the fluid is assumed to have the same density. The results of case 4-7 are very similar, indicating that the difference in density from 500 kg/m^3 to 1000 kg/m^3 has a limited influence on the

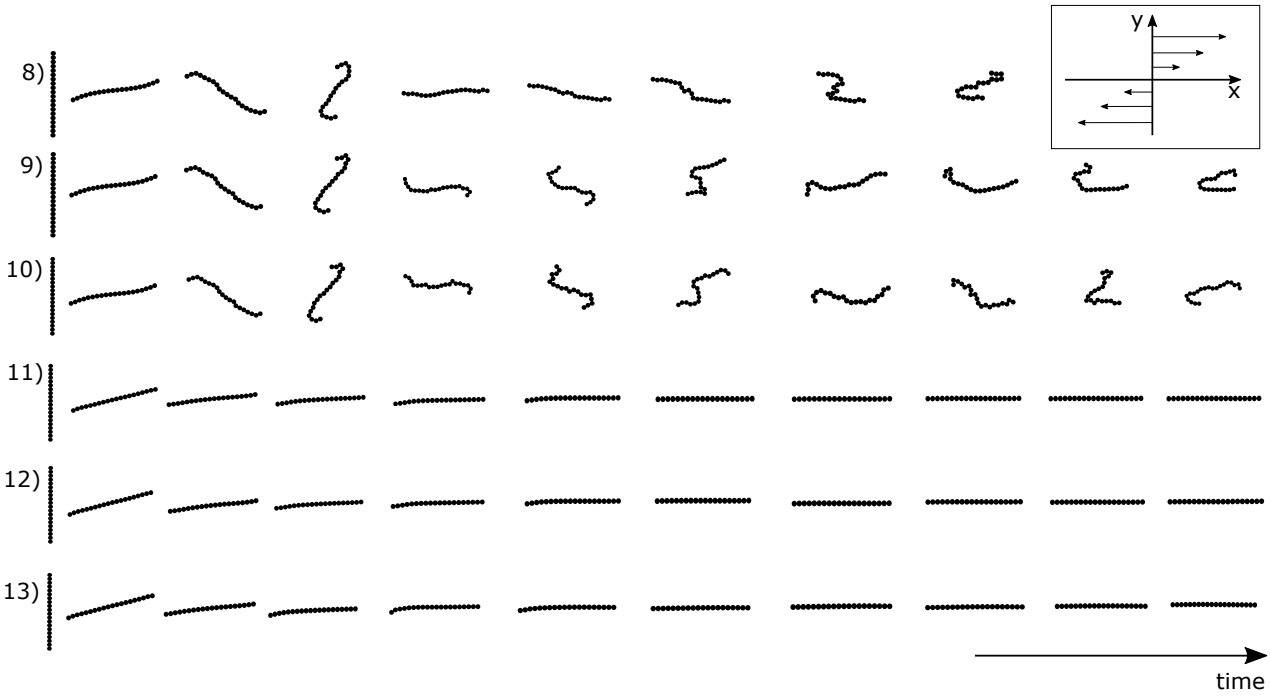

Figure 7. Development of the fiber shape with time in the different cases. The time interval between each image in a case is 1 s.

Table 1. Properties of the simulated fibers.

Fiber Simulation Cases					
Case	Density [kg/m^3]	Stiffness [N/m^3]	Segments [-]	Diameter [m]	Length [m]
1	5000	$1e^9$	50	0.0025	0.125
2	5000	$1e^8$	50	0.0025	0.125
3	5000	$1e^7$	50	0.0025	0.125
4	500	$1e^9$	50	0.0025	0.125
5	500	$1e^8$	50	0.0025	0.125
6	500	$1e^7$	50	0.0025	0.125
7	1000	$1e^9$	50	0.0025	0.125
8	5000	$1e^9$	20	0.0025	0.050
9	5000	$1e^8$	20	0.0025	0.050
10	5000	$1e^7$	20	0.0025	0.050
11	500	$1e^9$	20	0.0025	0.050
12	500	$1e^8$	20	0.0025	0.050
13	500	$1e^7$	20	0.0025	0.050

results. However, comparing to cases 1-3, with a fiber density of 5000 kg/m^3 and same range of fiber stiffness, the difference due to change in density is obvious, as the motion of the fibers in case 4-7 resembles the orbit of a rigid fiber until the fiber is parallel to the flow direction. After this, the fiber motion is similar to a coiled orbit with self entanglement. Case 4-6 differ in the fiber stiffness from $1e^7$ to $1e^9$. But this change in fiber stiffness is not evident from the results.

The motion of the fibers formed by 20 fiber segments, illustrated in Fig. 7, is very similar to the fiber formed of 50 segments for the first 5 s. Both for a fiber density of 500 and 5000 kg/m^3. This indicates that the number of segments forming the fiber is of small importance in this case. However, there are significant differences between fibers of 20 and 50 segments after 5 s of the simulation. This may be caused by a significant change in fiber aspect ratio, when reducing the number of fiber segments. The diameter of the fiber is kept constant at 2.5 mm in all simulations and consequently the aspect ratio of the fiber changes when the number of spherical segments forming the fiber is reduced from 50 to 20. A more direct comparison of the influence of fiber density and stiffness is presented in Fig. 8 and 9.

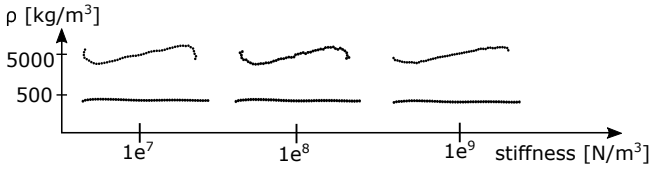

Figure 8. Comparison of fibers formed by 50 segments after 4 s.

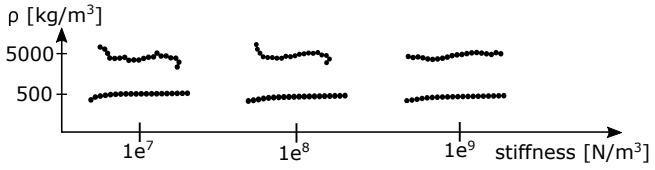

Figure 9. Comparison of fibers formed by 20 segments after 4 s.

The figures illustrate the shape of the fiber after 4 s of the simulation. It is seen from both Fig. 8 and 9 that the fiber stiffness slightly changes the motion of the fiber. Furthermore, a significant difference is evident with a change of fiber density from 500 to 5000 kg/m^3.

3. CONCLUSION

The software EDEM for DEM and the software ANSYS Fluent for CFD were used to simulate fibers in shear flow with a two-way coupling between fiber and fluid, to identify the importance of the fiber properties on the motion of the fiber in this flow condition.

A change in fiber density from 500 to 5000 kg/m^3 leads to a significant change in the fiber motion in shear flow. With a fiber density of 5000 kg/m^3 the motion of the fiber resembles the springy or snakelike orbit type reported in literature. In the case of a fiber density of 500 kg/m^3 the motion is more similar to rigid orbiting. However, in the case of 50 particle segments, this motion changes to coiled orbiting.

Changing the stiffness of the bonds between the particles from 1e^7 to 1e^9 only has a very limited influence on the results. A change in the number of particles forming the bond, from 50 to 20 gives similar results in the first half of the simulated time, but the difference between the results may be caused by the change in fiber aspect ratio.

This study has presented a qualitative comparison of fiber motion of fibers with different properties as well as comparison to fiber orbit types presented in literature. In order to determine if the built-in bond model and coupling in EDEM and ANSYS Fluent is applicable for clogging simulations, careful experimental validation of the motion of fibers with specific properties is needed. Furthermore, settling experiments or similar must be conducted for a model of a piece of textile. However, the presented results of fiber motion in shear flow, are similar to results presented in literature. This is promising for the future application of coupled CFD-DEM to model fiber motion and later simulation of clogging effects in wastewater pumps.

4. FUTURE WORK

The presented simulation of fibers in shear flow is the first step towards developing a framework for simulation of clogging effects in wastewater pumps. In order to accomplish this, experimental validation of both the coupling between CFD and DEM and the bond model in DEM for this application must be conducted. Based on the results of the validation, development and implementation of a new formulation of drag and DEM bonds may be necessary.

ACKNOWLEDGMENTS

This work is funded by Grundfos in cooperation with the Department of Energy Technology in Aalborg University.

REFERENCES

[1] C.S. Peskin. The immersed boundary method. *Acta Numerica*, 11:479–517, 2002.

[2] S. Sathe and T. Tezduyar. Modelling of fluid-structure interactions with the space-time finite elements: Contact problems. *Computational Mechanics*, 43(1):51–60, 2008.

[3] S.W. Attaway, M.W. Heinstein, and J.W Swegle. Coupling of smooth particle hydrodynamics with the finite element method. *Nuclear Engineering and Design*, 150(2-3):199–205, 1994.

[4] A.L. Jensen, H. Sørensen, L. Rosendahl, and F. Lykholt-Ustrup. Towards simulation of clogging effects in wastewater pumps: A review of the state-of-the-art in cloth modelling and challenges in the simulation of clogging effects. *ASME-JSME-KSME 2015 Joint Fluids Engineering Conference*, pages 2543–2549, July, 2015.

[5] P.A. Cundall and O.D.L. Strack. A discrete numerical model for granular assemblies. *Geotechnique*, 29:47–65, 1979.

[6] D.O. Potyondy and P.A. Cundall. A bonded-particle model for rock. *International Journal of Rock Mechanics and Mining Sciences*, 41:1329–1364, 2004.

[7] Y. Guo, C. Wassgren, B. Hancock, W. Ketterhagen, and J. Curtis. Validation and time step determination of discrete element modelling of flexible fibers. *Powder Technology*, 249:386–395, 2013.

[8] O.L. Forgacs and S.G. Mason. Particle motions in sheared suspensions. *Journal of Colloid Science*, 14:473–491, 1959.

[9] S. Yamamoto and T. Matsuoka. A method for dynamic simulation of rigid and flexible fibers in a flow field. *The Journal of Chemical Physics*, 98:644–650, 1993.

[10] C.F. Schmid, L.H. Switzer, and D.J. Klingenberg. Simulations of fiber flocculation: Effects of fiber properties and interfiber friction. *J. Rheol.*, 44:781–809, 2000.

[11] S.B. Lindström and T. Uesaka. Simulation of the motion of flexible fibers in viscous fluid flow. *Physics of Fluids*, 19:113307, 2007.

[12] C. Kloss, C. Goniva, A. Hager, S. Amberger, and S. Pirker. Models, algorithms and validation for opensource dem and cfd-dem. *Progress in Computational Fluid Dynamics*, 12(2/3):140–152, 2012.

[13] A. Salinas and J.F.T Pittman. Bending and breaking of fibers in sheared suspensions. *Polymer Engineering and Science*, 21:23–31, 1981.

[14] S. Ergun. Fluid flow through packed columns. *Chemical Engineering Progress*, 48:89–94, 1952.

[15] C.Y. Wen and Y.H. Yu. Mechanics of fluidization. *Chemical engineering progress symposium*, 62:100–111, 1966.

[16] R. Di Felice. The voidage function for fluid-particle interaction systems. *International Journal of Multiphase Flow*, 20:153–159, 1994.